http://dx.doi.org/10.21577/0103-5053.20180022

J. Braz. Chem. Soc., Vol. 00, No. 00, 1-12, 2018.
Printed in Brazil - ©2018 Sociedade Brasileira de Química

Article

Selective Adsorption of Au^{III} from Aqueous Solution Using 2,5-Dimercapto-1,3,4-thiadiazole Modified Persimmon Tannin

Sijing Zhang,[a] Yongliang Ji,[a] Fengjiao Ao,[a] Yongping Wang,[b] Junxue Zhao*[c] and Shuangli Chen[a]*

[a]*School of Science, Xi'an University of Architecture and Technology, 710055 Xi'an, China*

[b]*Shaanxi Provincial Academy of Environmental Science, 710061 Xi'an, China*

[c]*School of Metallurgical Engineering, Xi'an University of Architecture and Technology, 710055 Xi'an, China*

A one-pot synthesized persimmon tannin (PT)-based novel biosorbent modified with 2,5-dimercapto-1,3,4-thiadiazole (DMTD) was prepared for the selective adsorption of Au^{III} from aqueous mixtures. The synthesized biosorbent was designated as DMTD-PT and characterized using elemental analysis, zeta potential, Fourier transform infrared (FTIR) spectroscopy and X-ray photoelectron spectroscopy (XPS). The batch adsorption experiments in a model electronic waste leachate revealed that both DMTD-PT and PT had poor affinity for coexisting base metal ions, however, DMTD-PT and PT adsorbed 97.7 and 32.7%, respectively, of Au^{III} with an initial Au^{III} concentration of 78.0 mg L^{-1} in the mixtures with a dosage of 2.5 g L^{-1} each at pH 3.0 at ambient temperature. The adsorption results indicate the superior selectivity of DMTD-PT for Au^{III} compared to that of PT. The continuous column experiments further proved that DMTD-PT can be used to separate Au^{III} from aqueous mixtures. The maximum adsorption capacity of DMTD-PT for Au^{III} was determined to be 0.42 mmol g^{-1}. A kinetic study in combination with XPS and FTIR analyses of fresh and spent DMTD-PT further revealed that the potential biosorption mechanism can be attributed to the collaboration of electrostatic interactions and coordination.

Keywords: persimmon tannin, 2,5-dimercapto-1,3,4-thiadiazole, modification, selective adsorption, Au^{III}

Introduction

In the current information age, a growing amount of electronic waste from all sorts of abandoned electronic gadgetry creates environmental problems. However, it also provides an important secondary resource for extracting precious metals, because such waste generally contains higher concentrations of precious metals than those in even the richest ores.[1]

Hydrometallurgical methods are currently used more often to recover precious metals than pyro-metallurgy, which has encountered huge environmental challenges. However, compared to coexisting base metals, precious metals in both leachates and industrial effluents are still in very low concentrations. Conventional hydrometallurgical methods suffer from poor economy, and thus, biosorption, which uses various kinds of waste biomass, is well-recognized as a promising technology for the recovery of precious metals in an economical and eco-benign way.[2] Such a technology is also vitally crucial in terms of sustainable development because it would undoubtedly decrease the consumption of virgin materials and energy.[3]

Over the past decade, persimmon peels and residues, whose main composition is persimmon tannin (PT),[4] have attracted a great deal of attention among waste agricultural byproducts because of the plentiful resources and moderate conditions for chemical modification.[4] Relevant work has mainly focused on grafting amine- and thiourea (TU)-based modifiers on the PT matrix [5-7] to improve both adsorption capacity and selectivity for precious metals. It is imperative to develop new modifiers to provide more choices for modifying biosorbents for various purposes. In this context, guided by the structure-property relationship, 2,5-dimercapto-1,3,4-thiadiazole (DMTD) grafted PT (denoted as DMTD-PT) was synthesized using a one pot method and used for the selective recovery of gold from

*e-mail: 834630684@qq.com; zhaojunxue1962@126.com

model electronic waste leachate in the presence of coexisting base metal ions. To the best of our knowledge, we are the first to report such modifier to modify a biosorbent. As a member of heterocyclic thiadiazole derivatives, DMTD has been used in a wide variety of applications in fields such as agricultural, pharmaceuticals and materials chemistry.[8] Because of the structure and composition of DMTD, it is expected that DMTD-PT should have superior selectivity for adsorption of Au^{III} because the possible bonding sites of the diazole N and sulfydryl S provide feasibility for Au^{III} to become coordinated with the ligating N and S atoms.

This work examines the adsorption behaviors of DMTD-PT for Au^{III} from model electronic waste leachate. The adsorption thermodynamics were studied to determine the thermodynamic feasibility of biosorption. The adsorption kinetics study, Fourier transform infrared (FTIR) spectroscopy and X-ray photoelectron spectroscopy (XPS) analysis were used to elucidate the biosorption mechanism. DMTD-PT-packed column experiments were also used to evaluate the potential applicability of DMTD-PT as a candidate material for the selective recovery of gold from industrial effluents in an efficient, low-cost and eco-benign manner.

Experimental

All the chemical reagents used in the experiments were analytical grade (Sinopharm Chemical Reagent Shaanxi Co. Ltd.) and used without further purification. The crude PT was kindly donated by a local planter in the suburb of Xi'an. The stock solution of Au^{III} was prepared by dissolving $HAuCl_4 \cdot 4H_2O$ in 0.1 mol L^{-1} HCl and was used in single component adsorption experiments. The model electronic waste leachate containing Ni^{II}, Zn^{II}, Cu^{II}, Pb^{II} and Au^{III} for multi-component adsorption tests was prepared by dissolving corresponding base metal nitrates and tetrachloroaurate(III) tetrahydrate in 0.1 mol L^{-1} HCl solution. TU was used to prepare elution solution. Diluted HCl and NaOH were used to adjust the solution pH required. Other reagents used in the experiments include epichlorohydrin, methanol, potassium carbonate, DMTD and *N*,*N*-dimethylformamide (DMF).

Preparation of DMTD-PT

Because PT is partially soluble in water,[5] crude PT was first washed with deionized water to remove impurities and water soluble components. It was then dried in a convection oven at 353 K for 24 h, after crushing and sieving with 150 mesh. The obtained clean PT powder was collected for future use.

To chemically modify PT, DMTD was grafted onto the PT matrix via polyphenolic groups using epichlorohydrin as a cross-linker to further enhance the adsorption capacity and stability of PT. The resulting biosorbent was denoted DMTD-PT and the one pot synthesis method is shown in Scheme 1.

First, 7.2 g of PT powder was put into a 250 mL three-necked round-bottom flask and 7.0 g of DMTD, 0.8 g of K_2CO_3, 20 mL of epichlorohydrin, and 70 mL of DMF were then added. The pH was then adjusted to 11.0 with 1.0 mol L^{-1} NaOH, and the solution was kept to 323 K under a reflux condenser with continuous stirring for 12 h. The resulting DMTD-PT was centrifuged and then washed with methanol to remove residues of epichlorohydrin; it was further washed with deionized water to neutralize it. The DMTD-PT was dried in a convection oven at 323 K for 10 h and then crushed and stored in a bottle for future use.

Characterization of the biosorbents

The chemical properties of the biosorbents were characterized by Fourier transform infrared spectroscopy (FTIR, Shimadzu IRPrestige-21) by means of KBr disk technique. For convenience, the spectra of the sample were displayed in transmittance. The surface charge was measured

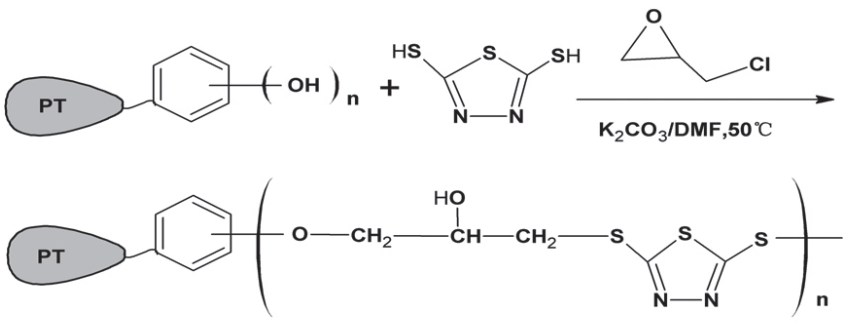

DMTD-PT

Scheme 1. Synthesis route for DMTD-PT. Hypothetical structure is shown, where PT stands for matrix of persimmon tannin.

by zeta potentiometer (Malvern ZEN1590). Six folds of PT suspensions with varying pH values (1.0-6.0) were used to measure zeta potential. Each PT suspension was prepared by dispersing 50 mg of powder sample into 30 mL deionized water, the pH of suspensions was adjusted with diluted HCl and NaOH solutions, and 10 mL of suspensions were loaded into the sample cell to measure zeta potential of PT, and zeta potential of modified derivative DMTD-PT at different pH was measured likewise. The elemental composition (i.e., C, H, N, S) of the biosorbents was determined by elemental analysis (Elementar Vario EL III) while the specific surface area was obtained by nitrogen physisorption (Micromeritics ASAP 2460). The total organic carbon (TOC) was analyzed on a TOC analyzer (Elementar Vario TOC cube analyzer) to evaluate the soluble organic carbons in the solution. A 10 mg of dried biosorbent was put into a 25 mL of conical flask and 10 mL of deionized water was added, the resulting mixture was then adjusted to pH 3.0 and shaken for 12 h in a shaker bath before measuring TOC of the filtrate. Surface analyses of the fresh and spent DMTD-PT were accomplished by X-ray photoelectron spectroscopy (XPS, Thermo Scientific K-Alpha) using a monochromatic Al X-ray source (1486.6 eV) at 350 W (25 mA ,14 kV) and a vacuum of 1×10^{-8} Torr operating in the constant analyzer energy (CAE) mode. The powder sample was slightly dusted on adhesive tape and carefully mounted for analysis. A low-energy electron flood gun was used to compensate the XPS-induced surface charging effects. The data were plotted with respect to the binding energy, which was referenced to the C1s line (284.6 eV) corresponding to adventitious carbon. The curve deconvolution of the observed spectra was fitted with the XPS peak fitting program.

Adsorption and separation experiments

Batch experiments of single and multi-metallic adsorption were carried out at room temperature (298 ± 2 K) in a shaker bath using 0.10 g of each PT and DMTD-PT with 40 mL of aqueous solutions in 100 mL conical flasks. Both the initial and final concentrations of the metallic ions in the solution were analyzed using an atomic absorption spectrophotometer (Thermo Scientific S SERIES-AA). Standard solutions were used for calibration before each set of analyses. The adsorption capacity, q_e (mg g^{-1}), was calculated using equation 1:

$$q_e = \frac{(C_0 - C_e) \cdot V}{m} \quad (1)$$

where C_o (mg L^{-1}) and C_e (mg L^{-1}) are the initial and final metal concentrations, respectively. V (L) is the solution volume and m (g) is the mass of the adsorbent.

The adsorption selectivity of the biosorbents for Au^{III} was demonstrated using a penta-component aqueous mixture of Au^{III}-Ni^{II}-Zn^{II}-Cu^{II}-Pb^{II}, and the composition was similar to that of the electronic waste leachate reported by Gurung *et al*.[6] The contents of Au^{III}, Ni^{II}, Zn^{II}, Cu^{II} and Pb^{II} in the model solution were 78.0, 600.8, 18.1, 7725.0 and 240.2 mg L^{-1}, respectively. The solution pH was adjusted to approximately 3.0 for the convenience of subsequent experiments.

The percent removal, η (%), of the metallic ions (equation 2) was determined via atomic absorption spectroscopy.

$$\eta\,(\%) = \frac{(C_0 - C_e)}{C_0} \times 100 \quad (2)$$

Continuous column tests

The continuous column tests were carried out using a small glass column with the height of 26.0 cm and internal diameter 0.80 cm to evaluate the possibility of DMTD-PT for selective adsorption of Au^{III} from a penta-component system in the presence of coexisting metallic ions with higher concentration. In the experiment, 0.4 g of DMTD-PT was dipped into deionized water for pretreatment for several hours before it was mounted in the glass column, then the fixed bed packed with DMTD-PT was first permeated with deionized water for 2 h and then successively followed by diluted HCl (pH 3.0) for 10 h. The model electronic waste leachate (pH 3.0) with certain concentrations of Cu^{II}, Zn^{II}, Pb^{II}, Ni^{II} and Au^{III} was penetrated upward through the packed bed at a constant flow rate of 5.0 cm^3 h^{-1} using a peristaltic pump (BT100S, Baoding Leifu, China). The effluent was periodically sampled and analyzed at hourly intervals by means of a fraction collector (SBS-100, Shanghai Huxi, China) to determine the residues of various metallic ions in the effluent by using atomic absorption spectrophotometer. The bed height of DMTD-PT was 0.90 cm with the volume of 0.45 cm^3 in this study, and the liquid hourly space velocity (LHSV) was 11.1 h^{-1}.

Generally, TU has stronger affinity for precious metal species than surface functional groups on the biosorbent, and it can thus act as a coordination agent to coordinate loaded precious metal species, TU has thus often been used as a high efficiency eluting solution to make precious metals elute from spent adsorbents. This has already been confirmed in relevant studies.[9-11] In the present study, after the loaded Au^{III} was saturated, the DMTD-PT packed bed was first washed with deionized water for 2 h, and then the adsorbed metallic ions were eluted with a solution of acidic TU (0.5 mol L^{-1} TU in 0.5 mol L^{-1} HCl) with an elution rate

of 10 cm^3 h^{-1} using a peristaltic pump operated as described above. The eluted solution was also periodically sampled and analyzed likewise at hourly intervals. After the elution of the adsorbed metals, the DMTD-PT was regenerated and used for the next cycle.

For the samples, the experiments were performed in triplicates. For each set of data analyzed, the mean values and standard errors were determined and used to show error bars in relevant figures.

Results and Discussion

Biosorbent characterization

FTIR spectra and TOC analysis

Figure S1 (Supplementary Information (SI) section) plots the infrared spectra of PT and DMTD-PT. The peak at 3423 cm^{-1} is attributed to the O–H stretching vibration, and this indicates that PT has a large amount of hydroxyl groups, whereas the peak at 1636 cm^{-1} in PT spectrum is assigned to the stretching vibrations of C=O. The peak at 1406 cm^{-1} arises from the stretching vibrations of the aromatic ring. The peaks at 1247 and 1059 cm^{-1} are attributed to symmetrical and asymmetrical C–O–C stretching vibrations.[6] These peak positions are consistent with the reported literature.[6]

After grafting DMTD, significant changes were observed. The peak that corresponds to the O–H stretching vibration at 3423 cm^{-1} shifted to 3428 cm^{-1}, the band was broader, and the intensity was slightly weaker; these observations indicate that cross-linking occurred at the hydroxyl group. The peak that corresponded to the C=O stretching vibration shifted from 1636 to 1630 cm^{-1}. The peak at 1406 cm^{-1} (C=C stretching vibration of the aromatic ring) shifted to 1441 cm^{-1}, indicating a structural change in the aromatic ring because of modification. The peak at 1372 cm^{-1} is attributed to the symmetrical bending vibration of C–H in $–CH_3$ and the peak at 1511 cm^{-1}, which is attributed to the C=N stretching vibration, is typical of a diazole ring.[12,13] In addition, the broad band at 1047 cm^{-1} is a combination band of C–O–C and C–S, indicating that DMTD was grafted onto PT.

TOC analysis can provide an indication of the water-soluble organic matter of biosorbents. The TOC values of PT and DMTD-PT were 22.30 and 8.50 mg L^{-1}, respectively, at pH 3.0. Thus, the aqueous solubilities of PT and DMTD-PT were both relatively low with respect to the adsorbent dose of 2.5 g L^{-1} used in this study, and thereby both PT and DMTD-PT were suitable for use as biosorbents.

Zeta potential of PT and DMTD-PT

Figure 1 plots the zeta potential of PT and DMTD-PT at different pH values.

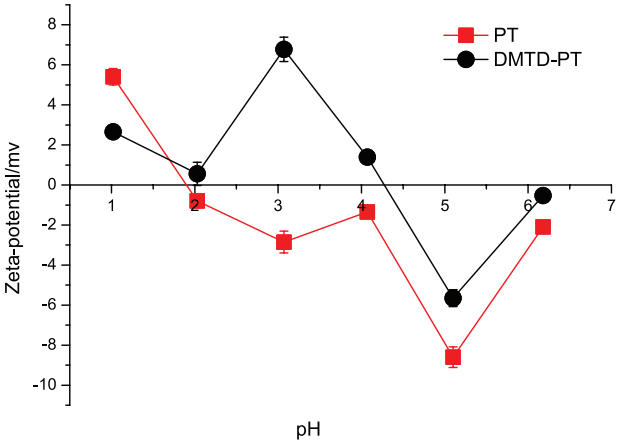

Figure 1. Zeta potential of PT and DMTD-PT at different pH.

The PT has an isoelectric point of ca. 1.9, while DMTD-PT shows an isoelectric point of ca. 4.3, which is higher than that of PT due to the introduction of DMTD. At pH value below that of the isoelectric point, the surface of the biosorbent is positively charged due to the formation of protonation sites, and is thereby beneficial to attract the anions in the solution via electrostatic interaction. Similarly, at pH value above that of the isoelectric point, the surface of the adsorbent is negatively charged due to the deprotonation of the functional groups, and is thus beneficial to attract the cations. Thus, the adsorption process would be facilitated if the solution pH was properly adjusted in terms of the metal species present.

Elemental analysis and Brunauer-Emmett-Teller (BET) surface area

IR spectra revealed qualitative information regarding the immobilization of functional groups on the PT surface, and such information was quantitatively corroborated via elemental analysis. The elemental compositions and BET surface areas of PT and DMTD-PT are all given in Table 1.

As shown in Table 1, the S and N contents in DMTD-PT are significantly higher than those in PT, and this confirms the successful grafting of S-containing and N-containing functional groups on the PT surfaces. Nitrogen physiosorption results show that the BET surface areas of PT and DMTD-PT were only 0.40 and 1.38 m^2 g^{-1}, respectively; in other words, both PT and DMTD-PT are nearly nonporous, and similar findings were also reported by Gurung *et al.*[14] This implies that the change in the Gibbs free energy of the surface was not the dominant driving force for the adsorption process, and thus, it is anticipated

Table 1. Elemental composition and BET surface area of PT and DMTD-PT

Biosorbent	Element / (wt.%)				N density[a] / (mmol g^{-1})	S density[a] / (mmol g^{-1})	BET surface area / (m^2 g^{-1})
	C	H	N	S			
PT	44.67	5.42	0.87	0.67	0.62	0.21	0.40
DMTD-PT	46.14	5.25	2.15	2.57	1.54	0.80	1.38

[a]This data was calculated based on the contents of nitrogen and sulfur determined from elemental analysis; PT: persimmon tannin; DMTD: 2,5-dimercapto-1,3,4-thiadiazole; BET: Brunauer-Emmett-Teller.

that the soft ligating sites of S and N atoms grafted on DMTD-PT have a key role in Au^{III} coordination.

Adsorption behavior of PT and DMTD-PT towards Au^{III} in single component solution

The effects of biosorbent dose and solution pH were studied to determine the optimal conditions for biosorption of gold ions. The experiments were performed at ambient temperature (298 K) unless otherwise specified.

Effect of biosorbent dose

The dose of the biosorbent greatly impacts the biosorption process. The effects of the biosorbent dose on the adsorption percentage and capacity for Au^{III} was plotted, and the plots are shown in Figure 2.

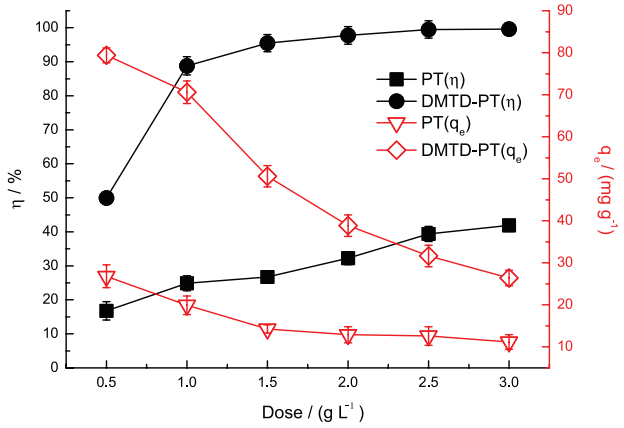

Figure 2. Effect of biosorbent dose on adsorption of Au^{III} (pH = 3.0, t = 12 h, $C_0(Au^{III})$ = 80 mg L^{-1}).

The adsorption percentage increased with the amount of added biosorbent. A higher dose is equivalent to an increase in the surface binding sites, which in turn facilitate adsorption. However, adsorption capacity (that is, the amount of adsorbed solute *per* unit mass of biosorbent) decreases with an increase in the biosorbent dose. A high biosorbent dose means there is a relative lack of solute available to cover the binding sites on the surface, and this implies a low solute adsorption.[15,16] In addition, as reported by Gadd *et al.*,[17] the competitive adsorption and mutual interference between binding sites at a high biosorbent dose also lowers the adsorption capacity of the biosorbents. Thus, to utilize the biosorbents efficiently and economically, both the adsorption percentage and adsorption capacity must be taken into account. A dose of 2.5 g L^{-1} for each PT and DMTD-PT were used herein and this dose was optimal for both the adsorption percentage and capacity. Also, it is clear from Figure 2 that DMTD-PT has superior adsorption capacity compared to that of PT at the same dosage.

Effect of the solution pH

The species of metals in solution are greatly dependent on pH,[18] and thus, the solution pH can affect both the dissociation state of the binding sites and the aqueous chemistry of the metal adsorbed in terms of coordination, redox potentials and hydrolysis.[19] Figure 3 shows plots of the Au^{III} adsorption at different values of initial pH on PT and DMTD-PT.

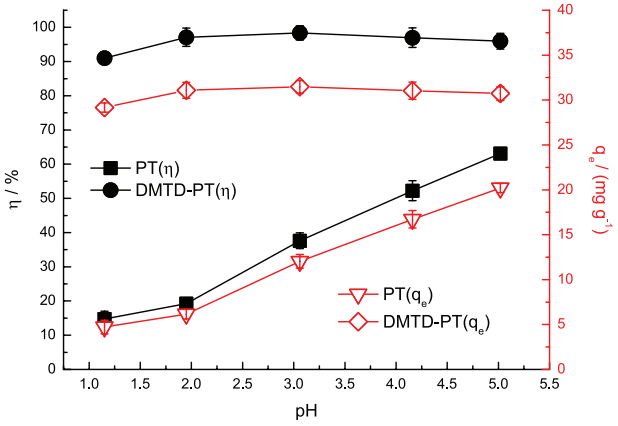

Figure 3. Effect of pH on adsorption of Au^{III} (t = 12 h, biosorbent dose = 2.5 g L^{-1}, $C_0(Au^{III})$ = 80 mg L^{-1}).

As shown in Figure 3, for DMTD-PT, when the pH was lower than that of the isoelectric point, DMTD-PT had relatively higher Au^{III} adsorption because the positively charged surface (as a result of protonation of the N-functional groups on the surface) was beneficial for attracting $AuCl_4^-$ via electrostatic interactions. However, when the pH was higher than that of the isoelectric point,

Au^{III} adsorption on DMTD-PT slightly decreased because the negatively charged surface of the adsorbent (as a result of deprotonation) repelled the adsorption of $AuCl_4^-$ via electrostatic interactions.

The above results are generally consistent with the zeta potential results (Figure 1). However, the changes in adsorption capacity are fairly low in the pH range of 1.0-5.0, and this indicates that the electrostatic interactions are not dominant during the adsorption process. This is especially true for the case of PT, because the adsorption capacity is not correlated with the zeta potentials. Also, as clear from Figure 3, DMTD-PT has a superior adsorption capacity to that of PT at the same pH, and this indicates that the adsorption property of DMTD-PT was significantly improved, and 98.3% of Au^{III} was adsorbed at pH 3.0. Thus, it was determined that an initial pH of 3.0 is suitable for the adsorption experiments. It is worth pointing out that the pH used in the experiments was initially adjusted and was found to change slightly in the first 2 h of the experiment. Specifically, the pH varied from 3.0 to 2.8 and then remained nearly unchanged thereafter, and this was possible because of the dissociation (to some extent) of polyphenol groups on the PT matrix.

Adsorption kinetics

The adsorption kinetics were studied in a single system of Au^{III} at ambient temperature to gain deep insight into the adsorption behaviors and the mechanism of DMTD-PT and PT with respect to Au^{III}.

As seen in Figure 4, the amount of adsorbed Au^{III} first increased dramatically in the initial stage (0-1 h), and then the increase was less pronounced thereafter (1-12 h) before equilibrium was achieved in approximately 12 h. The rapid Au^{III} adsorption in the initial stage was probably caused by the abundant availability of vacant active adsorption sites on the surface. After that period, it becomes gradually harder for the remaining vacant sites to be covered because of repulsive forces between adsorbed gold ions on the surface and those in bulk phase.[20] The equilibrium adsorption percentages of PT and DMTD-PT for Au^{III} are 37.3 and 98.2%, respectively, corresponding to adsorption capacities of 11.9 and 31.4 mg g^{-1}, respectively. Thus, the adsorption property of the chemically modified DMTD-PT was significantly improved.

The adsorption kinetics of Au^{III} uptakes by DMTD-PT and PT was further studied by applying the pseudo-second-order model,[21] which is now probably the most frequently used kinetic model to depict adsorption kinetics at the solid/solution interfaces.

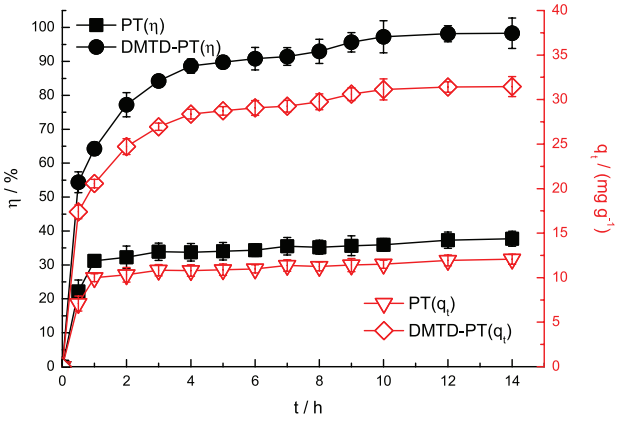

Figure 4. Adsorption kinetics of PT and DMTD-PT towards Au^{III} in single system (pH = 3.0, biosorbent dose = 2.5 g L^{-1}, $C_0(Au^{III})$ = 80 mg L^{-1}).

The linear expression of pseudo-second-order equation is given below as equation 3:

$$\frac{t}{q_t} = \frac{1}{k_2 q_e^2} + \frac{1}{q_e} t \quad (3)$$

where q_e and q_t (mg g^{-1}) are the adsorption capacities at equilibrium and time t (h), and k_2 (g mg^{-1} h^{-1}) is the rate constant of the pseudo-second-order adsorption process. k_2, q_e and correlation coefficients (R^2) could be obtained via the intercept and slope from linear plots of t/q_t *versus* t (as shown in Figure S2, SI section).

The linear fitted results and kinetic parameters are shown in Table 2. The R^2 suggested that adsorption process of DMTD-PT and PT towards Au^{III} fitted the pseudo-second-order model quite well, and the adsorption capacities from this model also well matched those obtained from experiments.

Table 2. Adsorption kinetic parameters of Au^{III} onto PT and DMTD-PT

Biosorbent	Pseudo-second order		
	k_2 / (g mg^{-1} h^{-1})	q_e / (mg g^{-1})	R^2
PT	0.2212	11.99	0.9984
DMTD-PT	0.0493	32.64	0.9988

PT: persimmon tannin; DMTD: 2,5-dimercapto-1,3,4-thiadiazole; k_2: rate constant of the pseudo-second-order adsorption process; q_e: adsorption capacity at equilibrium; R^2: correlation coefficient.

Gold separation from a multi-components system

As described in Experimental section, the biosorbents were further studied for the separation of Au^{III} from a model electronic waste leachate of Au^{III}-Ni^{II}-Zn^{II}-Cu^{II}-Pb^{II} at a pH of 3.0. As shown in Table 3, in this penta-component solution, the adsorption percentages of the tested coexisting metallic base ions using PT and DMTD-PT were both

Table 3. Adsorption percentages of biosorbents in Au^{III}-Ni^{II}-Zn^{II}-Cu^{II}-Pb^{II} system at pH 3.0

Metallic ion	C_0 / (mg L^{-1})	PT		DMTD-PT	
		C_e / (mg L^{-1})	η / %	C_e / (mg L^{-1})	η / %
Au^{III}	78.0	52.5 ± 1.5	32.7 ± 1.9	1.8 ± 1.4	97.7 ± 1.8
Ni^{II}	600.8	593.0 ± 6.5	1.3 ± 1.1	582.5 ± 5.9	3.0 ± 1.0
Zn^{II}	18.1	17.8 ± 0.3	1.7 ± 1.7	17.9 ± 0.2	1.1 ± 1.1
Cu^{II}	7725.0	7607.5 ± 70.1	1.5 ± 0.9	7730.5 ± 65.5	0 ± 0.8
Pb^{II}	240.2	235.0 ± 3.6	2.2 ± 1.5	229.2 ± 3.3	4.6 ± 1.4

PT: persimmon tannin; DMTD: 2,5-dimercapto-1,3,4-thiadiazole; η: percent removal; C_0: initial concentration; C_e: equilibrium concentrations of the metal ions in aqueous solution.

relatively lower, and PT, in particular, exhibited poor affinity for Au^{III}. This is consistent with similar findings in the single component system. In contrast, DMTD-PT had much better selectivity than that of PT over base metal ions in the penta-component system.

Thus, the adsorption percentage of PT only reached 32.7%, which is lower than that (37.3%) obtained in the single Au^{III} system at a comparable concentration. In contrast, DMTD-PT achieved Au^{III} removal of 97.7% under similar conditions, and this was very close to that (98.2%) obtained in the single Au^{III} system at comparable concentrations. These findings indicated that Au^{III} can be selectively separated from coexisting base metal ions using DMTD-PT.

The larger affinity of DMTD-PT towards Au^{III} *versus* other coexisting metallic ions allowed a selective Au^{III} biosorption process and its separation from multi-component systems. From Pearson's classification, Au^{III} is a soft acid, and the functional moieties of DMTD-PT are rich in soft base species, this is why DMTD-PT has superior selectivity for Au^{III}.

Adsorption isotherms and thermodynamics of Au^{III} on DMTD-PT

Adsorption isotherms of Au^{III} on DMTD-PT

To assess the adsorption property of the biosorbents, the maximum adsorption capacities of Au^{III} on DMTD-PT at different temperatures were determined using the Langmuir model of adsorption isotherms, as stated in equation 4.

$$\frac{C_e}{q_e} = \frac{1}{q_{max}b} + \frac{C_e}{q_{max}} \quad (4)$$

where C_e (mg L^{-1}) is the concentration of Au^{III} remaining after adsorption equilibrium, q_e (mg g^{-1}) is the corresponding mass of Au^{III} adsorbed *per* unit mass of the adsorbent, q_{max} (mg g^{-1}) is the maximum mass of Au^{III} adsorbed *per* unit mass of the adsorbent, and b (L mg^{-1}) is the Langmuir constant related to the energy of adsorption. The isotherm was established by determining C_e and q_e with various tested initial concentrations of Au^{III} at pH 3.0. The Langmuir adsorption isotherm plots of q_e *versus* C_e are shown in Figure 5.

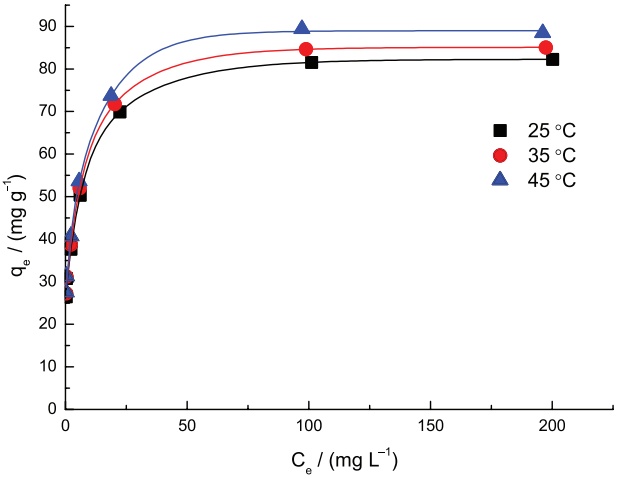

Figure 5. Langmuir adsorption isotherms of Au^{III} on DMTD-PT (pH = 3.0, biosorbent dose = 2.5 g L^{-1}, t = 12 h).

The adsorption capacity increased with an increase in temperature, indicating that the adsorption process of Au^{III} on DMTD-PT was endothermic. However, upon increasing the temperature from 298 to 318 K, the maximum adsorption capacities of DMTD-PT for Au^{III} only increased slightly, and this implies that temperature did not have a significant impact on the adsorption process. Thus, the biosorption can be carried out at ambient temperature. The values of the Langmuir constant b and the values of q_{max} are listed in Table 4; these values were obtained from the intercept and slope, respectively, of the linear Langmuir adsorption isotherm plots of C_e/q_e *versus* C_e (plots not shown).

The high regression coefficient values suggest that the experimental data fitted the Langmuir isotherm model quite well, and this indicates a typical monolayer type of adsorption process. Further, DMTD-PT had a superior adsorption capacity (equivalent to 0.42 mmol g^{-1}) for Au^{III} and had a comparable adsorption capacity as that of the reported adsorbents of thiourea-modified Amberlite XAD

Table 4. Langmuir isotherm parameters of Au^{III} on DMTD-PT

Temperature / K	q_{max} / (mg g^{-1})	b / (L mg^{-1})	R^2
298	83.17	0.4259	0.9995
308	86.06	0.4433	0.9994
318	89.68	0.4644	0.9996

q_{max}: maximum mass of Au^{III} adsorbed *per* unit mass of the adsorbent; b: Langmuir constant related to the energy of adsorption; R^2: correlation coefficient.

resin[22] (0.35 mmol g^{-1}) and Duolite GT-73[23] (0.58 mmol g^{-1}). However, it was lower than that of bisthiourea-modified BTU-PT (5.18 mmol g^{-1}),[6] and this is probably caused by the significant difference in the N and S contents of the biosorbents.

Thermodynamic parameters of biosorption

The changes in Gibbs free energy ($\Delta G^{\ominus}$), enthalpy ($\Delta H^{\ominus}$) and entropy ($\Delta S^{\ominus}$) of the biosorption process were studied to evaluate the thermodynamic feasibility and to prove the effectiveness of Au^{III} adsorption on DMTD-PT.

The biosorption process of Au^{III} on the biosorbent can be simply expressed using the following reversible heterogeneous equilibrium:

$$Au^{III}_{(aq)} + Biosorbent_{(s)} \rightleftharpoons Au^{III}\text{-}Biosorbent_{(s)}$$

The Langmuir constant b, which is the adsorption equilibrium constant, can be used to evaluate the thermodynamic parameters.[24-26] However, thermodynamically, the change in Gibbs free energy ($\Delta G^{\ominus}$) of the adsorption is related to the standard thermodynamic equilibrium constant ($b^{\ominus}$) via equation 5:

$$\Delta G^{\ominus} = -RT \ln b^{\ominus} \quad (5)$$

where R is the gas constant (8.314 J mol^{-1} K^{-1}), T is the absolute temperature (K), and the units of $\Delta G^{\ominus}$ are J mol^{-1}. The standard thermodynamic equilibrium constant ($b^{\ominus}$) is a dimensionless quantity.

Thus, instead of the Langmuir constant b (which is an experimental equilibrium constant), $b^{\ominus}$ should be used to calculate the change in the Gibbs free energy. $b^{\ominus}$ is determined using equation 6:

$$b^{\ominus} = b\, c^{\ominus} \quad (6)$$

where b is the Langmuir adsorption equilibrium constant (L mol^{-1}) and $c^{\ominus}$ is the standard concentration ($c^{\ominus}$ = 1.0 mol L^{-1}). $b^{\ominus}$ can be expressed using the van't Hoff equation (equation 7):

$$\ln b^{\ominus} = -\frac{\Delta G^{\ominus}}{RT} = -\frac{\Delta H^{\ominus}}{RT} + \frac{\Delta S^{\ominus}}{R} \quad (7)$$

$\Delta H^{\ominus}$ and $\Delta S^{\ominus}$ are obtained, respectively, from the slope and intercept of the linear plot of ln $b^{\ominus}$ *versus* 1/T (Figure S3).

The thermodynamic parameters are listed in Table 5. The negative value of $\Delta G^{\ominus}$ shows that biosorption of Au^{III} on DMTD-PT is spontaneous and the positive value of $\Delta H^{\ominus}$ suggests that the process is endothermic.

Table 5. Adsorption thermodynamic parameters of Au^{III} onto DMTD-PT

Temperature / K	$b^{\ominus}$	$\Delta G^{\ominus}$ / (kJ mol^{-1})	$\Delta H^{\ominus}$ / (kJ mol^{-1})	$\Delta S^{\ominus}$ / (J mol^{-1})
298	83902	–28.11	3.40	105.68
308	87330	–29.17		
318	91487	–30.22		

$b^{\ominus}$: standard thermodynamic equilibrium constant; $\Delta G^{\ominus}$, $\Delta H^{\ominus}$, $\Delta S^{\ominus}$: changes in Gibbs free energy, enthalpy and entropy of the adsorption, respectively.

The entropy change ($\Delta S^{\ominus}$) of the adsorption process depends upon two counteracting effects. On one hand, the diffusion of Au^{III} from bulk solution to the biosorbent surface would make the system more ordered and thus lead to the entropy of the system to decrease, while on the other hand, the surface of biosorbents underwent some structural changes during the adsorption, i.e., some water molecules adsorbed on the surface were replaced by Au^{III}. In this process, the translational entropy gained by released water molecules surpasses that lost by the adsorbed Au^{III}, thus increasing the randomness of the system.[27] It is clear, if the latter effect prevails over the former one, the overall entropy change ($\Delta S^{\ominus}$) would be positive, indicating randomness increased at the solid/solution interface during the biosorption, DMTD-PT adsorption towards Au^{III} is the right example for such a case.

Packed bed column adsorption and elution experiment

The prominent selectivity of DMTD-PT towards Au^{III} has been already proved by the batch adsorption experiments in the Au^{III}-Ni^{II}-Zn^{II}-Cu^{II}-Pb^{II} model electronic waste solutions. The feasibility of DMTD-PT to selectively enrich and recover Au^{III} from the same penta-component system was then evaluated by continuous column mode followed by elution. Breakthrough curve can intuitively reflect the adsorption relationship between the mobile phase and stationary phase in column adsorption process, and also serve as the basis for adsorption operating and controlling at industrial scale. Figure 6a displays the

breakthrough curves of the metallic ions under investigation over a DMTD-PT-packed column. As shown in Figure 6a, rapid breakthroughs were observed for Zn^{II}, Pb^{II}, Cu^{II} and Ni^{II} ions, thereby indicating that these coexisting metallic ions passed through the packed bed quickly without being adsorbed on DMTD-PT. Unlike these coexisting metals, a zigzag breakthrough curve was obtained for Au^{III}, which was indicative of a breakthrough adsorption ($C_t/C_0 = 0.1$) on the DMTD-PT-packed bed, occurring at 256 bed volumes (BV, equivalent to 23 h) and saturation being reached at 444 BV (40 h). These results indicated that DMTD-PT has a strong affinity towards Au^{III} which, in turn, facilitates the separation of Au^{III} from the coexisting base metals under continuous operation. The saturation adsorption capacity towards Au^{III}, calculated from the breakthrough curves (29.9 mg g^{-1}), was slightly lower than the equilibrium adsorption capacity which could be calculated from Table 3 in the batch experiments (30.48 mg g^{-1}). This difference can be mainly ascribed to a synergistic effect caused by: (*i*) the competitive adsorption of the various metallic ions; (*ii*) the lack of time for metallic ions to contact with the biosorbent and (*iii*) the channeling flow phenomenon.[6]

After the loaded Au^{III} got saturated, DMTD-PT-packed bed was eluted with 0.5 mol L^{-1} TU in 0.5 mol L^{-1} HCl to enrich and recover the loaded Au^{III}. Figure 6b showed the elution curve of the adsorbed Au^{III}. It can be seen that Au^{III} was eluted with a preconcentration factor of 10.2 within 2 h, and 96.7% of adsorbed Au^{III} was eluted within 6 h, suggesting that the elution was quite efficient.

Regeneration and reusability of DMTD-PT

The properties of DMTD-PT for its reusability and stability were assessed by the successive adsorption/elution cycle experiments in continuous column mode. As described in Experimental section, the penta-component Au^{III}-Ni^{II}-Zn^{II}-Cu^{II}-Pb^{II} acidic solutions flowed by the DMTD-PT-packed column till loaded Au^{III} got saturated. Au^{III}-loaded DMTD-PT was then eluted with 0.5 mol L^{-1} TU in 0.5 mol L^{-1} HCl till it was regenerated. The regenerated DMTD-PT was subsequently fitted with diluted HCl (pH = 3.0) for 2 h prior to the next cycle of adsorption. This process was similarly repeated 5 times to perform consecutive adsorption/elution cycles, and the results were illustrated in Figure S4 (SI section). As clearly shown, even after five repeated cycles, 85.9% of adsorbed Au^{III} was still recovered. DMTD-PT thus exhibited qualified durability and better adsorption characteristics toward Au^{III}. Consequently, DMTD-PT could be potentially used to recover gold from various gold-containing industrial effluents.

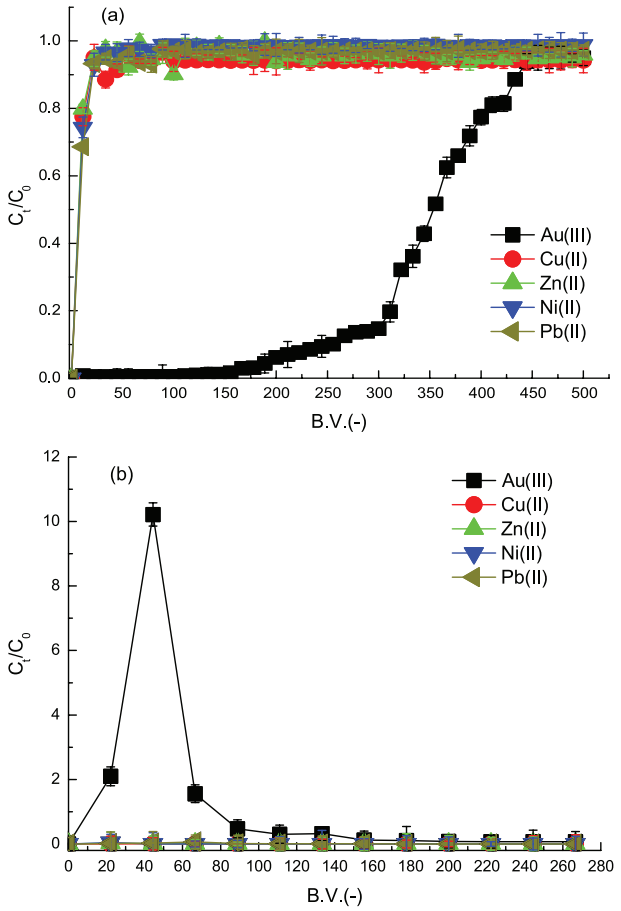

Figure 6. Breakthrough curves (a) and elution curves (b) of metallic ions on DMTD-PT in Au^{III}-Ni^{II}-Zn^{II}-Cu^{II}-Pb^{II} system. Feed concentrations of metallic ions (mg L^{-1}): Au^{III} = 78.0; Ni^{II} = 600.8; Zn^{II} = 18.1; Cu^{II} = 7725.0 and Pb^{II} = 240.2 with flow rate 5.0 cm^3 h^{-1}; eluent = 0.5 M thiourea in 0.5 M HCl with elution rate 10.0 cm^3 h^{-1}.

Presumable biosorption mechanism

As shown in Figure 1, under acidic conditions (that is, for pH values lower than the isoelectric point) the nitrogen atoms of DMTD-PT are easily converted into positively charged centers as a result of protonation, and this favors the adsorption of the anionic $AuCl_4^-$ via electrostatic interactions.

Most of the functional groups that contain N and S atoms can act as mono-, bis-, and polydentate ligands to form complexes with Au^{III}. Because Au^{III} is a soft acid, coordination between Au^{III} and functional groups containing soft donor atoms is reasonable. Hence, as shown in Scheme 2, it is logical to propose that the presumable mechanism of Au^{III} biosorption on DMTD-PT can be principally attributed to the collaboration of electrostatic interactions via ion exchange (Scheme 2b) and coordination via groups containing N and S atoms (Scheme 2c).

From elemental analysis results (Table 1), it is easy to calculate that the S grafted on DMTD-PT was 0.59 mmol g^{-1}.

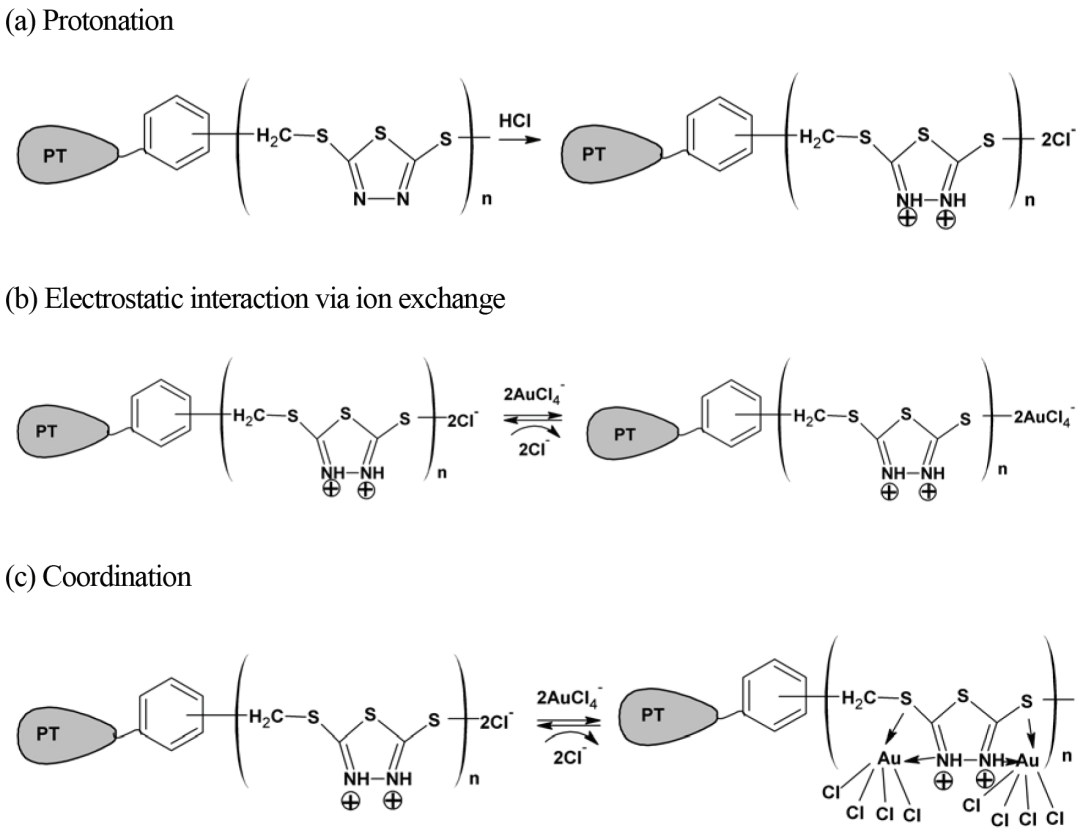

Scheme 2. Proposed mechanism of Au^{III} adsorption on DMTD-PT. (a) Protonation; (b) electrostatic interaction via ion exchange; (c) coordination.

As shown in Scheme 2c, two-thirds of the S grafted on DMTD-PT was coordinated with Au^{III}. Specifically, the maximum Au^{III} adsorption capacity was roughly 0.39 mmol g^{-1}, which is very close to the value obtained from the Langmuir adsorption isotherm (0.42 mmol g^{-1}) that was determined via analysis of experimental data. This indicates that coordination is the main mechanism for Au^{III} adsorption on DMTD-PT. Incidentally, a similar coordination structure was also proposed by Tiwari *et al.*[13] in a study of a DMTD-Au coordination polymer.

The FTIR spectra of fresh and Au^{III}-loaded DMTD-PT supported the proposed adsorption mechanism. As shown in Figure S5 (SI section), after adsorption of Au^{III}, significant changes were observed in the spectra of Au^{III}-loaded DMTD-PT. The peak at 1511 cm^{-1} that was ascribed to the C=N stretching vibration of a diazole ring shifted to 1524 cm^{-1}, and the stretching vibration of C–S at 1047 cm^{-1} shifted to 1049 cm^{-1}, indicating the involvement of N and S atoms in the coordination of Au^{III}, as depicted in Scheme 2c. The coordination changed the chemical environment around the functional groups, which in turn caused changes in the relevant peak wavelengths. This was indicated by the stretching vibration band of C=O that shifted from 1630 to 1655 cm^{-1} and the weak bending vibration of C–H in the aromatic ring that appeared at 1170 cm^{-1}.

XPS analyses of fresh and Au^{III}-loaded DMTD-PT also supported the proposed adsorption mechanism. XPS data for the C1s, N1s, S2p, and Au4f transitions of DMTD-PT and Au^{III}-loaded DMTD-PT are shown in Figure 7. As shown in Figure 7a, the broad C1s peak for DMTD-PT was deconvoluted into peaks that correspond to C=N (286.18 eV) and C–C (284.58 eV).[28] A slight increase in the C1s binding energy in C=N (286.48 eV) after Au^{III} adsorption on DMTD-PT indicates a potential interaction between Au^{III} and a functional group containing C=N. The adsorption of metallic ions influences both the local chemical environment and the entire hydrophobic and hydrophilic nature of the biosorbent,[29] and thereby, such adsorption affects the accessibility of active sites for biosorption.

A slight increase of the N1s binding energy (Figure 7b) was also observed after Au^{III} adsorption. The S2p band was deconvoluted (Figure 7c), and the main band at 163.88 eV was ascribed to C–S species.[13,28] The binding energy of this peak slightly increased after Au^{III} adsorption, and this suggests possible interactions between Au^{III} and S atoms. Typical peaks of Au4f5/2 (87.98 eV) and Au4f7/2 (84.28 eV)[13,28] were observed (Figure 7d), and these confirm the adsorption of Au^{III} on DMTD-PT.

Donation of electron pairs from S2p and N1s to the unoccupied orbital of Au^{III} to form a coordination

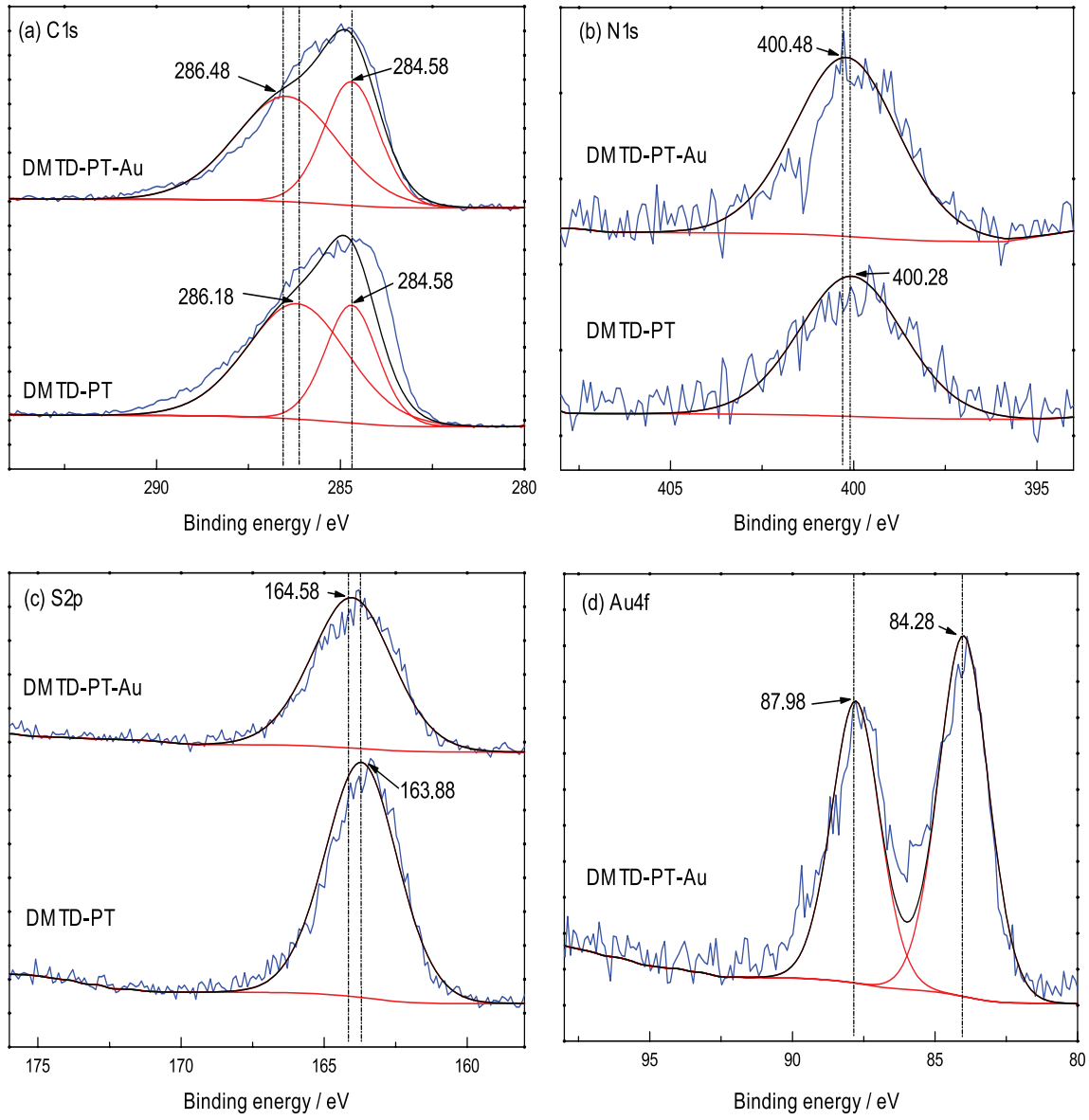

Figure 7. X-ray photoelectron spectra of fresh and Au^{III}-loaded DMTD-PT. (a) C1s; (b) N1s; (c) S2p and (d) Au4f.

compound during the biosorption process resulted in the atomic orbitals of S2p and N1s having a lower density of electrons. This, in turn, increased the binding energies of S2p and N1s in the Au^{III}-loaded DMTD-PT.

Conclusions

2,5-Dimercapto-1,3,4-thiadiazole ligands were grafted onto the matrix of persimmon tannin to prepare a persimmon tannin-based biosorbent. Elemental analysis and FTIR results confirmed the successful grafting of DMTD on PT. Adsorption experiments revealed that the ability of DMTD-PT to adsorb Au^{III} was greatly improved after chemical modification. Both DMTD-PT and PT had low affinity for coexisting base metallic ions in a model electronic waste leachate containing Au^{III}, Ni^{II}, Zn^{II}, Cu^{II} and Pb^{II}. Batch mode adsorption experiments indicated that, in the presence of coexisting base metals, DMTD-PT had both a higher adsorption percentage and selectivity for Au^{III} than PT. Continuous column tests with packed DMTD-PT further confirmed that Au^{III} was efficiently enriched and separated from acidic mixtures in the presence of coexisting base metals. A potential mechanism to elucidate the selective adsorption of Au^{III} on DMTD-PT was principally attributed to the collaboration of electrostatic interactions (via ion exchange) and coordination. In summary, DMTD-PT had superior adsorption capacity and selectivity for Au^{III}, and it can potentially be used as an efficient, low-cost, and eco-benign candidate material for the selective recovery of gold from various gold-containing industrial effluents.

Supplementary Information

Supplementary information (Figures S1-S5) is available free of charge at http://jbcs.sbq.org.br as a PDF file.

Acknowledgments

The authors are grateful for the financial support from the Natural Science Foundation of Education Department of Shaanxi Provincial Government (2013JK0873) and the National Natural Science Foundation of China (No. 51674185).

References

1. Cui, J.; Zhang, L.; *J. Hazard Mater.* **2008**, *158*, 228.
2. Das, N.; *Hydrometallurgy* **2010**, *103*, 180.
3. Cui, J.; Forssberg, E.; *J. Hazard Mater.* **2003**, *99*, 243.
4. Inoue, K.; Gurung, M.; Xiong, Y.; Kawakita, H.; Ohto, K.; Alam, S.; *Metals* **2015**, *5*, 1921.
5. Gurung, M.; Adhikari, B. B.; Khunathai, K.; Kawakita, H.; Ohto, K.; Harada, H.; Inoue, K.; *Sep. Sci. Technol.* **2011**, *46*, 2250.
6. Gurung, M.; Adhikari, B. B.; Kawakita, H.; Ohto, K.; Inoue, K.; Alam, S.; *Ind. Eng. Chem. Res.* **2012**, *51*, 11901.
7. Gurung, M.; Adhikari, B. B.; Alam, S.; Kawakita, H.; Ohto, K.; Inoue, K.; *Chem. Eng. J.* **2013**, *228*, 405.
8. Hu, Y.; Li, C. Y.; Wang, X. M.; Yang, Y. H.; Zhu, H. L.; *Chem. Rev.* **2014**, *114*, 5572.
9. Ricoux, Q.; Bocokić, V.; Méricq, J. P.; Bouyer, D.; Zutphen, S. V.; Faur, C.; *Chem. Eng. J.* **2015**, *264*, 772.
10. Awual, M. R.; Khaleque, M. A.; Ratna, Y.; Znad, H.; *J. Ind. Eng. Chem.* **2015**, *5*, 405.
11. Das, A.; Ruhela, R.; Singh, A. K.; Hubli, R. C.; *Sep. Purif. Technol.* **2014**, *125*, 151.
12. Zerzouf, A.; Keita, A.; Salem, M.; Essassi, E. M.; Roumestant, M. L.; Viallefont, P.; *C. R. Acad. Sci., Ser. IIc: Chim.* **1999**, *2*, 7.
13. Tiwari, M.; Gupta, S.; Prakash, R.; *RSC Adv.* **2014**, *49*, 25675.
14. Gurung, M.; Adhikari, B. B.; Alam, S.; Kawakita, H.; Ohto, K.; Inoue, K.; Harada, H.; *Chem. Eng. J.* **2013**, *231*, 113.
15. Tangaromsuk, J.; Pokethitiyook, P.; Kruatrachue, M.; Upatham, E. S.; *Bioresour. Technol.* **2002**, *85*, 103.
16. Zhang, S. J.; Ao, F. J.; Wang, Y.; Zhao, J. X.; Ji, Y.; Chen, S.; *J. Renewable Mater.* **2017**, *in press* DOI: 10.7569/JRM.2017.634154.
17. Gadd, G. M.; White, C.; de Rome, L. In *Biohydrometallurgy*; Norris, P. R.; Kelly, D. P., eds.; Science and Technology Letters: Kew, 1988, p. 421.
18. Esposito, A.; Pagnanelli, F.; Vegliò, F.; *Chem. Eng. Sci.* **2002**, *57*, 307.
19. Fiol, N.; Villaescusa, I.; Martinez, M.; Miralles, N.; Poch, J.; Serarols, J.; *Sep. Purif. Technol.* **2006**, *50*, 132.
20. Hameed, B. H.; Tan, I. A. W.; Ahmad, A. L.; *Chem. Eng. J.* **2008**, *144*, 235.
21. Ho, Y. S.; McKay, G.; *Process Biochem.* **1999**, *34*, 451.
22. Zuo, G.; Muhammed, M.; *React. Polym.* **1995**, *24*, 165.
23. Iglesias, M.; Anticó, E.; Salvadó, V.; *Anal. Chim. Acta* **1999**, *381*, 61.
24. Gupta, V. K.; Jain, C. K.; Ali, I.; Sharma, M.; Saini, V. K.; *Water Res.* **2003**, *16*, 4038.
25. Hsu, T. C.; Yu, C. C.; Yeh, C. M.; *Fuel* **2008**, *87*, 1355.
26. Cheng, L.; Hou, C.; Zhang, B.; Liu, G.; *RSC Adv.* **2016**, *6*, 114361.
27. Fan, H. T.; Wu, J. B.; Fan, X. L.; Zhang, D. S.; Su, Z. J.; Yan, F.; Sun, T.; *Chem. Eng. J.* **2012**, *198-199*, 355.
28. Moulder, J. F.; Stickle, W. F.; Sobol, P. E.; Bombein, K. D.; *Handbook of X-ray Photoelectron Spectroscopy*; Perkin-Elmer Corp: Eden Prairie, 1992.
29. Chen, X.; Lam, K. F.; Mak, S. F.; Yeung, K. L.; *J. Hazard Mater.* **2011**, *186*, 902.

Submitted: October 23, 2017
Published online: February 14, 2017